Biological effect of four iron-containing materials developed for nanoremediation on green alga *Chlamydomonas* sp.

[a]Nhung H. A. Nguyen, [b]Nadia R. von Moos, [b]Vera I. Slaveykova*, [c]Katrin Mackenzie, [d]Rainer U. Meckenstock, [e]Silke Thűmmler, [f,1]Julian Bosch, and [a]Alena Ševců*

[a]Technical University of Liberec; Institute for Nanomaterials, Advanced Technologies and Innovation; Faculty of Mechatronics, Informatics and Multidisciplinary Studies; Studentská 2, 461 17 Liberec, Czech Republic, nhung.nguyen@tul.cz, alena.sevcu@tul.cz

[b]University of Geneva, Faculty of Sciences, Earth and Environmental Sciences, Department for Environmental and aquatic sciences, Uni Carl Vogt, 66 Bvd Carl Vogt, 1211 Geneva, Switzerland, vera.slaveykova@unige.ch, nadia.vonmoos@immerda.ch

[c]Helmholtz Centre for Environmental Research GmbH-UFZ, Permoserstraße 15, 04318 Leipzig, Germany. katrin.mackenzie@ufz.de

[d]University of Duisburg-Essen, Biofilm Centre, Universitätsstr. 5, 45141 Essen, Germany. rainer.meckenstock@uni-due.de

[e]Verfahrensentwicklung Umweltschutztechnik Recycling GmbH, Chemnitzer Straße 40,09599 Freiberg, Germany. Silke.Thuemmler@mvtat.tu-freiberg.de

[f]Helmholtz Zentrum München, Ingolstädter Landstraße 1, D-85764 Neuherberg, Germany.

[1]Present address: Intrapore UG, Katernberger Str. 107, 45327 Essen, Germany. julian.bosch@intrapore.com

*corresponding authors: alena.sevcu@tul.cz; vera.slaveykova@unige.ch

Abstract

The further emerging broader nanoremediation strategy for *in-situ* groundwater treatment requires ecotoxicological evaluation of newly developed materials. Four particle types containing Fe in different speciation and offering various modes-of-action were subject to ecotoxicological studies using unicellular green alga of the genus *Chlamydomonas* sp. as a model test system. The tested particles were (i) FerMEG12 as pristine flakelike milled Fe(0) nanoparticle (nZVI), (ii) Carbo-Iron® as Fe(0)-nanocluster-containing activated carbon (AC) composite for contaminant reduction, (iii) Trap-Ox® Fe-BEA35 (Fe-zeolites) as Fe-doped zeolite and Nano-Goethite as 'pure' FeOOH. Biological effects associated to their intended and unintended release in the environment were studied. Number of algal cells, chlorophyll fluorescence, efficiency of photosystem II, membrane integrity and reactive oxygen species (ROS) generation were examined during exposure to 10, 50 and 500 mg L^{-1} of the particles for 2 h and 24 h and compared with unexposed controls. Results showed that the particles affect *Chlamydomonas* sp. depending on concentration, type of material and in a time-dependent manner. The effect on green alga decreased in the order: FerMEG12 > Carbo-Iron® > Fe-zeolites > Nano-Goethite. Particle aggregation and sedimentation were discussed to have contributed to the reduction in negative effects. A shading effect by the particles within the test systems was found to contribute to the observed effect when alga was exposed to high concentrations (500 mg L^{-1}) of FerMEG12 and Carbo-Iron. We found that the tested materials can be ranked as non-hazardous according to CEC. Nonetheless, they exhibit a potential to induce significant toxicity to tested alga at high concentrations >500 mg L^{-1}, which represents the concentration typically used for the suspension during the subsurface injection process. The presented findings contribute to enable the practical usage of particle-based nanoremediation in environmental restoration.

Keywords: biological effect, FerMEG12, Carbo-Iron, Trap-Ox Fe-zeolites, Nano-Goethite, *Chlamydomonas* sp.

Introduction

Iron-based materials possess a remarkable potential for the remediation of soil aquifers, groundwaters and cyanobacterial bloom control (Bardos et al., 2015; Ribas et al., 2016; Sharma et al., 2016). Alone numerous *in-situ* applications of zero-valent iron (ZVI) nanoparticles have proved that they are a powerful tool in the clean-up of chlorinated ethenes and toxic metal ions due to their high reductive capacity (Köber et al., 2014; Mueller et al., 2012). Further particulate materials containing Fe as Fe(0), Fe(II) and Fe(III) are emerging materials which support nanoremediation approaches where the Fe function is the reactive species as acting as reductant or sorbent for metals and metalloids, as support of microbiological contaminant degradation or as heterogeneous Fenton catalyst (Bardos et al., 2015; Mackenzie et al., 2016; Gillies et al., 2017).

The overall impact of Fe(0) nanoparticles on aquatic ecosystems due to their intended use but also accidental spills is still questionable (Bardos et al., 2015). However, also other nanomaterials have the potential to seriously affect aquatic microorganisms such as microalgae, primary producers that play a key role in healthy ecosystems (Adeleye et al., 2016; Klaine et al., 2008). While the element iron is an essential nutrient when present in small amounts, increased loading of Fe(II)/Fe(III) ions can rapidly accumulate in the cells of aquatic organisms, resulting in oxidative stress due to generation of oxide and hydroxide radicals via the Fenton reaction (Crane and Scott, 2012; Davies, 2000; Franqueira et al., 2000; Gillies et al., 2016). Moreover, ZVI nanoparticles show a strong affinity for cell surfaces, thus have the potential to physically damage bacterial or algal cells (Auffan et al., 2008; Lei et al., 2016).

A variety of Fe-containing materials has been developed in the European FP7 project NanoRem (Taking Nanotechnological Remediation Processes from Lab Scale to End User Applications for the Restoration of a Clean Environment, for more information see nanorem.eu) in order to provide new and improved materials for treatment of contaminated

76 environments, treat a broader contaminant spectrum and offer more cost effectiveness and
77 safety during transportation and application (Bardos et al., 2015). The nanoremediation
78 approach for *in-situ* generation of permeable reactive barriers or zones by particle subsurface
79 injection was up to now dominated by nanoiron-based approaches for contaminant reduction.
80 By introduction of other particles with different abilities, nanoremediation has been extended
81 to support bioremediation, advanced oxidation and sorption-assisted clean-up strategies in
82 permeable barriers. Three of the newly developed particles studied (FerMEG12, Carbo-Iron®
83 and Nano-Goethite) are field tested and commercially available while the Trap-Ox® particles
84 are at the premarket development state. FerMEG12 and Carbo-Iron® contain Fe(0) and were
85 designed to treat a wide range of organic pollutants by reduction (Köber et al., 2014;
86 Mackenzie et al., 2012). Carbo-Iron® in addition offers the combination of pollutant
87 adsorption at the AC grain. The Nano-Goethite particles coated by humic acid (coated
88 FeOOH) have been applied for stimulated microbial Fe reduction-based bioremediation of
89 BTEX (Bosch et al., 2010). Nano-Goethite shows superior mobility in soils and has been
90 designed for enhanced microbial Fe reduction for contaminant oxidation within the permeable
91 treatment zone. Trap-Ox® Fe-zeolites, were developed as *in-situ* Fenton-like catalyst for
92 remediation of groundwater contaminated with small organic molecules (Gonzalez-Olmos et
93 al., 2009). Specialty of the zeolite particles are their tuneable selective adsorption of
94 contaminant molecules by choosing the best fit in pore size and therefore a combination of
95 adsorption and treatment by advanced oxidation. The Fe function is provided by iron
96 exchange of Fe(II) against H^+.

97 With view on an upcoming application of the particles for water treatment, we assessed
98 the effect of FerMEG12, Carbo-Iron®, Nano-Goethite and Fe-zeolites towards green alga
99 *Chlamydomonas* sp., found in water and on soil by multiple biological end-points: number of
100 algal cells, chlorophyll fluorescence, quantum efficiency of photosystem II (PSII), membrane
101 integrity, and reactive oxygen species generation (ROS). The algae system was chosen as
102 system which is not necessarily associated to particle incorporation but contact effects to the

103 cell wall. As also shown by investigation of quantum dots, the algae system stands for particle
104 propagation within the food chain to invertebrates (Bouldin et al., 2008). The size and zeta-
105 potential were followed in the algal exposure media. This present study was conducted to
106 provide more ecotoxicity data for the four newly developed Fe materials and is seen as
107 amendment to other studies using further test systems, such as the currently published
108 ecotoxicity results of the same materials developed within the aforementioned EU-project
109 Nanorem (Hjorth et al., 2017).

110 **Materials and methods**

111 *Materials*

112 Four particle types were tested which are intended for subsurface application as suspensions.
113 Only Fe-zeolites did not require the aid of a stabilizer to form a stable suspension, in case of
114 Nano-Goethite a humic-acid coating and for the other two particles the addition of suspension
115 stabilizers, such as carboxymethyl cellulose, were needed for stabilisation of the suspension
116 during injection. The Fe-containing materials itself tested in this study were received as dry
117 powders and suspended according to the producers advices. The FerMEG12 was developed
118 by the firm UVR-FIA GmbH (Germany), Carbo-Iron® and Fe-zeolites by the Helmholtz
119 Centre for Environmental Research GmbH-UFZ (Germany), and the Nano-Goethite by the
120 Helmholtz Zentrum München HMGU/University of Duisburg-Essen (Germany).

121 *FerMEG12* are metallic nanoiron particles, which were produced mechanically using a two-
122 stage top-down process. Particles with a size of less than 40 µm were first generated by dry
123 milling and then finely ground by wet milling in bivalent alcohol. The resultant
124 nanostructured flake-shaped particles exhibit an average surface area of 13-18 $m^2\ g^{-1}$ (Köber
125 et al., 2014) and consist of approx. 80% ZVI.

126 *Carbo-Iron®* is a composite of ZVI-nanostructures embedded in AC particles of about 1 µm
127 in size. Carbo-Iron® was synthesised carbothermally following a wet impregnation step,

128 where the pores of the colloidal AC particles were filled with ferric nitrate (Bleyl et al., 2012).
129 Electron microscopy of the product after reduction indicates nZVI clusters of predominantly
130 $d_{Fe} \approx 50$ nm built into the AC grain (Mackenzie et al., 2012). The Carbo-Iron® particles are
131 composed of 20±1 wt% ZVI, 30.3±1.5 wt% Fe_{total} and 55±1 wt% C_{total} and have a specific
132 surface area between 550 and 650 m^2 g^{-1} (N_2-BET).

133 *Fe-zeolites* have a particle size of about 500 nm and are composed of 38 wt% silicon, 1.8 wt%
134 aluminium and 1.3 wt% Fe_{total} (Gillies et al., 2017). With a specific surface area of 602 m^2 g^{-1}
135 (N_2-BET) and water-filled pore effective density of $\rho \approx 1.7$ g cm^{-3}, the particles show
136 favourable sedimentation behaviour (i.e. 11 to 15 mm h^{-1}) (Gillies et al., 2016 and 2017;
137 Gonzalez-Olmos et al., 2013).

138 *Nano-Goethite* is produced using an industrial FeOOH precursor, ultrasonification and
139 coating with a layer of natural organic matter polymers which results in electro-steric
140 stabilisation (Bosch et al., 2010). The resultant particles have a specific surface area of 136 m^2
141 g^{-1} (N_2-BET). A stable stock suspension contains 100 g L^{-1} of Nano-Goethite with a mean
142 particle size of 400 nm.

143 A field-emission SEM (Zeiss Ultra Plus) was used to analyse the Fe-containing particles.
144 Samples were fixed to aluminium stubs using double-sided carbon tape and cleaned with RF
145 plasma (Evactron) for 10 min before image acquisition. For further details see the supporting
146 information section (Fig. S1).

147 *Characterisation of Fe materials in exposure media*

148 The hydrodynamic diameter of each particle type was determined for various suspension
149 concentrations (10, 50 and 500 mg L^{-1}) in the algal growth media by dynamic light scattering
150 (DLS) using a Malvern Zetasizer Nano ZS (Malvern Instruments, UK) with a 633 nm laser
151 source and a detection angle of 173°. The same instrument was used to measure
152 electrophoretic mobility, which was subsequently transformed to zeta potential using

153 Smoluchowski's approximation. Triplicate measurements for each sample in 30 s intervals
154 were carried out. Oxidation reduction potential (ORP) and pH were measured for all
155 suspensions at the beginning and the end of the toxicity tests using a standard multimeter
156 (WTW, Germany).

157 *Algal cultures and exposure conditions*

158 The *Chlamydomonas* sp. was obtained from the Biology Centre of the Czech Institute of
159 Hydrobiology, originally isolated from the Lipno reservoir. The algae were cultivated in
160 Guillard-Lorenzen medium (Guillard and Lorenzen, 1972) (Table S1) in an incubator
161 (PlunoTech, Czech Republic) with a 150 rpm shaker and temperature set to 22±2°C, light
162 intensity set to 1200 lux applying a light:dark regime of 14:8 hours. The culture was harvested
163 during its exponential growth phase and re-suspended in the exposure media to cell density of
164 1×10^{6} cells mL^{-1}.

165 The effect of the Fe-containing materials on *Chlamydomonas* sp. was tested by exposure to
166 10, 50 and 500 mg L^{-1} for 2 and 24 h. The experiments were carried out in fully light-
167 transmissive plastic vials containing 5 mL of *Chlamydomonas* sp. and the particle
168 suspensions. Negative controls without particles were run in parallel. The exposure
169 experiments were performed under the same conditions (light, temperature and agitation
170 regimes) as described for the stock algal culture. The possible effects due to shading and
171 sedimentation of particles were also considered, since high material concentrations produced
172 a deep, dark (FerMEG12 and Carbo-Iron®, Figs. S2, S3), skimmed milk-like (Fe-zeolites, Fig.
173 S3) or light brownish-red (Nano-Goethite, Fig. S3) coloured suspensions. After 2 h and 24 h
174 exposure, 250 µl sub-samples were taken and examined by flow cytometry (FCM) to assess
175 the effects of each nanomaterial on number of algal cells, cellular membrane integrity and
176 chlorophyll fluorescence. Oxidative stress (ROS) was detected using a Synergy HTX
177 fluorescence reader and the effect on the algal photosystem II was measured with an
178 AquaPen-C fluorometer.

179 *Determination of particle effects on membrane integrity*

180 A 250 µL aliquot of each sample was transferred to a Microtiter® 96-well flat-bottomed plate
181 and Sytox Green or propidium iodide (PI) fluorescent probes (Life Technologies,
182 Switzerland) were added to the sample at final concentrations of 1 µM and 7 µM,
183 respectively. These probes stain the DNA of affected cells by penetrating impaired cell
184 membranes. The plates were incubated in the dark for 20 minutes before FCM measurement.
185 Each algal suspension was then passed through a BD Accuri C6 Flow Cytometer (BD
186 Biosciences, USA) with a blue 488 nm excitation laser. Green fluorescence of Sytox Green
187 was measured using the 533/30 nm FL1 channel, red fluorescence of PI using the 585/40 nm
188 FL2 channel and red chlorophyll autofluorescence using the > 670 nm FL3 channel. Cells
189 treated in hot water (100 °C) for 15 minutes were used as a positive control (Fig. S4).
190 Unexposed algae stained with fluorescent probe signals were also included as a negative
191 control. One vial was covered with aluminium foil to create dark conditions mimicking the
192 shading effect caused by the dark colour of Fe materials. Data were analysed using CFlow
193 Plus software (BD Biosciences, USA). Determination of algal cell number and
194 autofluorescence; the percentage of cells with intact, unaffected membranes and cells labelled
195 by Sytox Green and PI (Cheloni et al., 2014) are all illustrated in the flow cytometry analysis
196 section (Figs. 1, S5).

197 *Determination of changes in number of algal cells*

198 Changes in the total number of algal cells was evaluated as cells $mL^{-1} = (N_{24h} - N_{2h}) / (24\ h -$
199 $2\ h)$; where N_{2h} is the number of cells after 2 h exposure to the particles and N_{24h} is the
200 number of cells after 24 h exposure. *Chlamydomonas* has a new generation approximately
201 every 24 h. The number of algal cells at the inoculation time 0 (0 h) and the time point 2 h (2
202 h) was be considered as similar.

203 *Flow cytometry analysis*

204 FCM is the reliable tool to study ecotoxicity of different materials on algae and used
205 according a standard procedure developed in Environmental Biogeochemistry and
206 Ecotoxicology, Earth and Environmental Science laboratory, Institute F.-A. Forel, multitude
207 of published papers using FCM for nanomaterials (Cheloni et al., 2014; von Moos et al.,
208 2015; Cheloni et al., 2015; Cheloni et al., 2016). The FCM tool was used to distinguish the
209 algal cells from the particle aggregates with similar size and to distinguish different
210 fluorescence from algal cells (*Chl*) (FL3). Sytox (FL1) and PI (FL2) were used as staining
211 markers (Fig. 1).

212 *Determination of the effects of particles on intracellular ROS generation*

213 Sub-samples of 200 µL were taken after 2 h, 4 h and 24 h and stained with carboxy-
214 H2DCFDA C-400 (Molecular Probes, Thermo Fisher Scientific Inc.). The intracellular ROS
215 staining procedure used followed that detailed in Szivák et al. (2009). Cells were treated with
216 H_2O_2 (final concentration of 100 mM) in preliminary test to verify the ROS staining
217 procedure. An algal culture without particles was used as a negative control. Fluorescence
218 was measured using a Synergy HTX plate reader (BioTek, USA) with excitation set at 485
219 nm and emission at 528 nm. The results were presented as the ratio between fluorescence
220 units (FU) in the presence of particles (FU_E) against FU for controls without particles (FU_0):
221 FU_E/FU_0.

222 *Determination of particle effect on photosystem II (PSII)*

223 Suspensions of the all particle types were added to the same algal cultures in 30 mL glass
224 flasks in order to achieve final concentrations of 50 and 100 mg $L^{-1}$of FerMEG12 and Carbo-
225 Iron®, and 50, 100 and 500 mg L^{-1} of Fe-zeolites and Nano-Goethite. An algal culture without
226 particles was used as a negative control and incubated in the dark as a mimic control for the
227 dark colour of the materials. Aliquots (2.2 mL) of each sample were taken immediately and
228 after 24 h incubation to determine the effect of the materials on the photosystem II quantum

229 yield (QY) using an AquaPen-C AP-C 100 fluorometer (PSI Ltd., Czech Republic). All
230 measurements were undertaken in triplicate. QY represents the ratio of variable fluorescence
231 ($F_v = F_m - F_0$) to maximum fluorescence (F_m), QY = F_v:F_m. It is used as a proxy of
232 photochemical quenching efficiency (Maxwell and Johnson, 2000). F_m was obtained by
233 applying illumination (3000 µmol photons m^{-2} s^{-1}) at 680 nm for a few seconds, with minimal
234 fluorescence (F_0) being the initial measurement at the minimum fluorescence level in the
235 absence of photosynthetic light.

236 *Optical microscopy*

237 Untreated *Chlamydomonas* cells (negative control), hot-water treated cells (positive control)
238 and cells exposed for 2 h and 24 h to the four Fe-containing materials (500 mg L^{-1}) were
239 visualized using an AxioImager microscope (Zeiss, Germany) equipped with an
240 AxioCamIcc1 digital camera and AxioVision SE64 software.

241 *Statistical analysis*

242 Differences in the effects observed for *Chlamydomonas* exposed to different concentrations of
243 the particles and for unexposed *Chlamydomonas* were tested using ANOVA and Dunnett's
244 test (GraphPad PRISM, USA). Significance levels were set at * $P < 0.05$, ** $P < 0.01$, and
245 *** $P < 0.001$.

246 **Results**

247 *Effect of Fe-containing particles on number of algal cells and cell morphology*

248 Generally it was observed, that the number of algal cells gradually decreased as
249 concentrations of the Fe-containing materials increased. At 500 mg L^{-1}, the algal number was
250 reduced to 4.4×10^2 cells mL^{-1} for FerMEG12 as well as Carbo-Iron® ($P < 0.001$), 1.1×10^4
251 cells mL^{-1} for Fe-zeolites ($P < 0.001$) and 4.9×10^4 cells mL^{-1} for Nano-Goethite (all $P < 0.01$)
252 comparing to unexposed control (8.7×10^4 cells mL^{-1}) and algal number in the dark without

253 particles (3.8×10^4 cells mL^{-1}, $P < 0.001$) (Fig. 2). Likewise, when algal cells were grown in
254 the presence of 50 mg L^{-1} of FerMEG12, the number of cells was also reduced significantly
255 ($P < 0.001$). Fe-zeolites and Nano-Goethite at 50 mg L^{-1} showed similar significant effect on
256 algal number ($P < 0.05$). In opposition, Carbo-Iron® showed no effect at this concentration. At
257 the lower particle concentrations of 10 mg L^{-1} for four types of particles, however, the algal
258 number was comparable with that for the untreated control culture (Fig. 2).

259 Microscopic analysis revealed that algal cells were trapped within the body of particle
260 agglomerates following short-term (2 h) exposure with FerMEG12 and Carbo-Iron® (Figs.
261 S6A, C). In addition, a palmeloid formation was observed when *Chlamydomonas* sp. was
262 exposed to Fe-zeolites and Nano-Goethite (Figs. S6E, G). Interestingly, after 24 h exposure
263 all algal cells tended to transfer from the agglomerate or palmeloid state to the dispersed
264 single cell state (Figs. S6B, D, F, H).

265 *Effect of Fe materials on algal chlorophyll fluorescence and PSII efficiency*

266 The percentage of cells with decreased chlorophyll fluorescence increased significantly after
267 2 h exposure to FerMEG12, Carbo-Iron® and Fe-zeolites at concentrations of > 10 mg L^{-1} and
268 to Nano-Goethite at concentrations of 500 mg L^{-1} (85.6%). A significant increase in
269 chlorophyll fluorescence ($P < 0.001$) was observed after 24 h exposure to particles at all
270 concentrations (Fig. 3). Exposure to 10 and 50 mg L^{-1} of Nano-Goethite had no significant
271 effect on algal chlorophyll fluorescence determined using FCM (Fig. 3). In the dark, algal
272 chlorophyll fluorescence was reduced to 92.0% ($P < 0.001$) after 24 h. The intensity of the
273 material's influence on chlorophyll florescence after 24 h exposure decreased in the order:
274 FerMEG12 > Carbo-Iron® > Fe-zeolites > Nano-Goethite.

275 The above observations were consistent with the effect of the particles on PSII QY (quantum
276 yield). PSII QY values for *Chlamydomonas* exposed to 10 mg L^{-1} of each particle type for 2 h
277 and 24 h were comparable with those for the control (Fig. 4). When cells were exposed to 50
278 mg L^{-1} of the milled metallic iron particle FerMEG12, however, a significant decrease in the

279 PSII QY was found in both short-term ($P < 0.01$) and longer-term exposure ($P < 0.05$). In
280 agreement with the observed decrease in cell growth and algal chlorophyll fluorescence, QY
281 was significantly inhibited following 2 h exposure to 50 mg L^{-1} of FerMEG12 and 500 mg L^{-1}
282 of Nano-Goethite. Carbo-Iron® (up to 50 mg L^{-1}) and Fe-zeolites (up to 500 mg L^{-1}) had no
283 significant effect on algal QY following 24 h exposure ($P > 0.3$; Fig. 4). While Nano-Goethite
284 had no significant effect on PSII efficiency after 24 h, the effect on QY was less pronounced.
285 In the dark, QY was slightly reduced after 2 h ($P < 0.05$) and significantly reduced after 24 h
286 ($P < 0.001$).

287 *Effect of Fe materials on cellular ROS generation and membrane integrity*

288 The studied ROS production in particle-treated *Chlamydomonas* sp. showed no clear trend
289 (Fig. 5). FerMEG12 caused a significant increase in ROS at 500 mg L^{-1} after 2 h, and at all
290 concentrations after 4 h. After 24 h, ROS formation was reduced at lower exposure
291 concentrations (10, 50 mg L^{-1}) to levels comparable with untreated cells, but remained higher
292 at 500 mg L^{-1}. For Fe-zeolites, ROS generation increased after 4 h and decreased slightly after
293 24 h, though remaining higher than the untreated control. Carbo-Iron®-induced ROS levels
294 increased rapidly when cells were exposed to 10 and 50 mg L^{-1} of the material, attaining a
295 maximum at 4 h. Enhanced ROS generation was not found at the highest Carbo-Iron®
296 concentrations (500 mg L^{-1}) at 4 h or 24 h exposure. Nano-Goethite at 500 mg L^{-1} resulted in
297 elevated ROS levels at all exposure duration. At lowest concentrations (10 mg L^{-1}), Nano-
298 Goethite generated ROS after 2 h, which increased after 4 h but was comparable with ROS in
299 untreated cells after 24 h (Fig. 5).

300 Furthermore, exposure to the particles induced a relatively weak effect on algal membrane
301 integrity (used as a surrogate of cell viability). In agreement with the observed decrease in cell
302 number and algal chlorophyll fluorescence, the percentage of cells with affected membrane
303 integrity was higher after 2 h than after 24 h exposure to all materials studied (Fig. 6). While
304 the percentage of algal cells with affected membranes was 30 to 40% for FerMEG12, 18% for

305 Carbo-Iron®, 29% for Fe-zeolites and 10% for Nano-Goethite at concentrations of 10 and 50
306 mg L^{-1} following a short-term exposure of 2 h, these percentages had all decreased to around
307 10% after 24 h exposure. Even at the highest concentration tested (500 mg L^{-1}), percentages
308 of cells with affected membrane integrity were moderate e.g. 39% for FerMEG12, 25% for
309 Carbo-Iron®, 25% for Fe-zeolites and 15% for Nano-Goethite. However, there was a
310 significant difference in the proportion of cells with damaged membranes after 2 h and 24 h
311 exposure to high (500 mg L^{-1}) particle concentrations.

312 *Characterisation of Fe-containing materials in algal exposure medium*

313 Nano-Goethite had the smallest average hydrodynamic (Z-average) size in the exposure
314 medium, ranging from 207 to 288 nm (Table 1). The Fe-zeolites Z-average was around 3.5
315 times higher than that for Nano-Goethite, ranging from 788 to 976 nm, while those for Carbo-
316 Iron® and FerMEG12 ranged from 1325 to 2874 nm and 3726 to 4973 nm, respectively. No
317 significant difference in Z-average size was observed at 2 h and 24 h after dispersion in the
318 algal exposure medium (Table 1). FerMEG12 and Nano-Goethite both displayed monomodal
319 size distributions, while Carbo-Iron® and Fe-zeolites both displayed bimodal number- and
320 scattered light intensity-based size distributions indicating formation of agglomerates (Fig.
321 S7).

322 Beside from the zeta potential of FerMEG12, which showed positive values (+ 5 mV) at high
323 concentrations (500 mg L^{-1}) in algal medium, all other values measured were mostly negative
324 (- 8 to - 35 mV) after 2 h (Fig. 7). Zeta potentials measured at the exposure times 2 h and 24 h
325 did not vary significantly. For all particle types, negative values were found which slightly
326 increased as material concentrations increased.

327 Growth medium pH values ranged between 7 and 8 for all *Chlamydomonas* samples
328 following the dispersion of Fe materials (Fig. S8A). In the presence of Carbo-Iron®, Fe-
329 zeolites and Nano-Goethite, pH values were comparable with those in the absence of NMs.
330 The pH of algal medium containing FerMEG12, however, increased to 8 at highest

concentrations (500 mg L^{-1}). ORP values for cultures without particles were in the range of +80 to +210 mV (Fig. S8B). In contrast, the ORP for the nZVI particle type FerMEG12 ranged between -200 and -300 mV at time 0, and between +80 and + 180 mV for all tested particle types at 24 h.

Discussion

The assessment of biological effect of four Fe-containing reactive particle types (FerMEG12, Carbo-Iron®, Fe-zeolites and Nano-Goethite) towards *Chlamydomonas* sp. was performed in relevant environmental concentrations of the materials (10 and 50 mg L^{-1}). A reference concentration (500 mg L^{-1}) simulating accidental spills of the injection suspension was also included into the studies. Suspensions containing up to 10 g L^{-1} of particles are usually injected during large-scale *in-situ* applications, such as reported for nZVI injection for treatment of chlorinated organic contaminants (Mueller et al., 2012; Soukupova et al., 2015). Following migration of *in-situ* applied nZVI suspensions within the treated aquifer or water body, the Fe concentrations are expected to decline to the range of mg L^{-1} or below (Mueller et al., 2012).

An integrated approach based on determination of multiple biological responses, involving the growth rate, chlorophyll autofluorescence and photosystem II (PSII) efficiency, membrane integrity and ROS generation, was applied to evaluate any possible effect of the new *in-situ* applicable materials containing different Fe species to green microalga, which is widely present in both aquatic and soil environments. The combination of the results demonstrated that the exposure to the studied Fe-containing particles induce significant reduction in growth of the green alga *Chlamydomonas* sp, which was found to be among the most sensitive species towards nanomaterials (Bondarenko et al., 2013); the effect being dependent on the type of nanomaterial, time and concentration applied.

355 Comparing different materials at higher exposure concentrations, their effects on the algal
356 growth decreased in the order FerMEG12 > Carbo-Iron® > Fe-zeolites > Nano-Goethite. The
357 observed trends are in agreement with the results of previous studies (Auffan et al., 2008; He
358 et al., 2008; Keller et al., 2012; Vardanyan and Trchounian, 2012; Velásquez et al., 2014).
359 Although the very strong agglomeration of FerMEG12 and Carbo-Iron® was observed in the
360 exposure medium, these materials induced strongest effect on alga. As depicted in Fig. S8,
361 algae seem to be trapped by the agglomerates of these two materials. In addition, the shading
362 is by all means caused by the dark colour of the dark-coloured materials (FerMEG12, Carbo-
363 Iron®) and light darkness (Nano-Goethite) when present at higher concentrations (500 mg L^{-1},
364 Fig. S2, S3). Simulating shading by the dark particles by shading the test vials in the dark
365 indeed reduced algal growth to 43% (3.8×10^4 cells) after 24 h compared with that for alga
366 grown in standard dark/light cycle conditions. Previous studies of nanomaterial toxicity to
367 algae have revealed that shading can considerably influence assessment of potential toxicity
368 (Hjorth et al., 2015; Sørensen et al., 2016). In one of the studies it was shown that ZVI
369 reduced algal growth by shading to a higher extend than by other toxicity mechanisms
370 (Schiwy et al., 2016). These observations are also consistent with the effect on chlorophyll
371 fluorescence and quantum efficiency of PSII in 2h exposure observed for Fe-containing
372 materials in the present study. Shaded algal cells need more chlorophyll to acquire enough
373 photons for photosynthesis (Nielsen and Jørgensen, 1968), hence they can rapidly synthesise
374 chlorophyll as an adaption to darker conditions (Schwab et al., 2011; Hjorth et al., 2015). In
375 the case of Nano-Goethite and Fe-zeolites, however, chlorophyll fluorescence and efficiency
376 of PSII increased after 24 h, indicating rapid recovery from the particle-induced stress. The
377 above observations were also consistent with the higher percentage of the ZVI present in the
378 materials (with FerMEG12 containing 80% ZVI and Carbo-Iron® containing 20% ZVI)
379 showing higher toxicity to *Chlamydomonas* sp. Indeed, the results in the literature for iron
380 nanoparticles demonstrated that the toxicity strongly depends on the percentage and the
381 surface coating of the nZVI used (El-Temsah et al., 2016; Keller et al., 2012). ZVI toxicity

382 can be also influenced by corrosion and transformation processes, ferrous ion release and
383 oxygen consumption (Chen et al., 2011; Zhu et al., 2012). FerMEG12 and Carbo-Iron®
384 possessed higher ZVI reactive characteristics, with ZVI capable of releasing dissolved Fe(II)
385 and penetrating cells, causing oxidative stress via the classic Fenton reaction (Lee et al., 2008;
386 Ševců et al., 2011). Moreover, ORP values in algal cultures treated with FerMEG12 (50 to
387 500 mg L^{-1}) ranged from -300 mV to -200 mV (Fig. S8B), suggesting that algal cells were
388 subjected to unfavourable reducing conditions in the growth medium in the beginning of the
389 experiment. These low ORP values could have negatively affected algal density (Wang et al.,
390 2014). There is no evidence that pH affected the algal cells, because it was within the optimal
391 growth range (pH 7 – 8) for *Chlamydomonas* (Messerli et al., 2005).

392 FerMEG12 could impair the cell membranes directly having a flake-like appearance with
393 rough, sharp edges and surfaces (Fig. S1). Moreover, the zeta-potential of FerMEG12
394 suspension reached values close to zero mV or positive values at concentrations of 500 mg L^{-1}
395 (Fig. 7), suggesting facilitated interaction of positively charges material surfaces with the
396 negatively charged surface of algal cells (Fig. S6A).

397 Furthermore, transition metals (such as the Fe investigated in the present study) which can
398 participate in one-electron oxidation-reduction reactions producing ROS can show direct toxic
399 effects to living organisms (Crane and Scott, 2012; Schiwy et al., 2016; Ševců et al., 2011).
400 As well as discussed for the ZVI particles, also Fe-zeolites and Nano-Goethite can release Fe
401 ions. The Fe-zeolites, a material developed to adsorb and oxidize organic pollutants
402 (Gonzalez-Olmos et al., 2013) are designed to generate hydroxyl radicals which would cause
403 most probably an increase in oxidative stress. However, the hydroxyl radicals will only be
404 generated during intended subsurface use with H_2O_2 addition. The algal cells formed
405 palmeloids with this particle type, which have previously been reported as indicative of
406 oxidative stress in *Chlamydomonas* cultures due to high ROS levels (Franqueira et al., 2000).
407 In accordance with our study, modified Fe(III)-zeolite inhibited *Chlamydomonas vulgaris*

408 growth, probably due to the formation of ROS (Pavlíková et al., 2010). Active defence
409 mechanisms against ROS are, however, a prerequisite for aerobic organisms such as algae
410 (Schwab et al., 2011; Cheloni et al., 2014). Our results showed ROS significantly increasing
411 within the first 4 h of exposure and then decreasing at lower particle concentrations,
412 suggesting that the algal cells were able to cope with the Fe-induced stress (Fig. 5). This trend
413 can be assigned to the decrease in free Fe(II) concentration released by particle leaching, due
414 to ongoing oxidation and precipitation of the anions under test system conditions and are
415 therefore withdrawn slowly from the algal cells. Similarly, for ZVI particles, passivation of
416 the iron surface by oxidation and precipitation leads to the same effect (Adeleye et al., 2013).
417 Moreover, the concentration of the particles being in direct contact with algae was
418 significantly reduced due to sedimentation of particle aggregates (Figs. S3, S7). This process
419 would inevitably happen in natural environments as well. Notably, the highest concentration
420 of each of the Fe-containing materials caused higher oxidative stress lasting until the end the
421 experiment, indicating inability of a certain part of the *Chlamydomonas* culture to effectively
422 defend ROS over 24 h. Previous studies have suggested that also the goethite mineral could
423 generate ROS via a Fenton-like reaction due to Fe ions released from the mineral grain (Kwan
424 and Voelker, 2003). Even though both non-ZVI particles Fe-zeolites and Nano-Goethite
425 generated cellular ROS, their levels were considerably lower than those in FerMEG12 and
426 Carbo-Iron® exposure reflecting the significant role of ZVI in induction of oxidative stress in
427 algal cultures. Of the studied particle types Nano-Goethite induced a weak alteration of algal
428 cell membrane integrity and chlorophyll fluorescence only at the highest concentrations of
429 500 mg L^{-1}. On a micro-scale, goethite is commonly found in natural environments and has
430 not previously been reported as toxic to microorganisms (Cooper et al., 2003).

431

Conclusions

Effects of Fe-containing particles which are newly developed for *in-situ* subsurface application to generate permeable reactive zones for groundwater remediation on green alga *Chlamydomonas* sp. were studied. The influence of increasing concentrations of the particles on algal number, chlorophyll fluorescence, quantum efficiency of PSII, ROS generation and membrane integrity was demonstrated together with their agglomeration behaviour and changes in their surface charge. For all biological responses found and tested materials, the determined effective concentration corresponding to alteration in 50% of the algal population was higher than 100 mg L^{-1}. This shows that all four Fe-containing particle types can be ranked as non-harmful to *Chlamydomonas* sp., classified according to the CEC median effect concentration corresponding to growth inhibition in 50% of the algal population EC_{50} > 100 mg L^{-1}. The shading effect from dark colour of materials was involved in this toxicity study. Moreover, at higher concentrations, the Fe-containing materials tended to rapidly agglomerate, which has to be regarded as their natural behaviour in the environment.

Acknowledgements

This research was supported by the European Union's Seventh Framework Programme for research, technological development and demonstration under grant agreement no. 309517. Further support was provided to N. Nguyen and A. Ševců from Ministry of Education, Youth and Sports CZ project no. LO1201, and the OPR&DI project - CZ.1.05/2.1.00/01.0005, and NanoEnvi project no. LM2015073. V. Slaveykova and N. von Moos received funding from the Swiss National Science Foundation - NRP 64, on the Opportunities and Risk of Nanomaterials, project no. 406440-131280.

Conflict of Interest

The authors declare that they have no conflict of interest.

456 **References**

457 Adeleye, A.S., Keller, A.A., Miller, R.J., Lenihan, H.S., 2013. Persistence of commercial
458 nanoscaled zero-valent iron (nZVI) and by-products. J. Nanoparticle Res. 15, 1–18.

459 Adeleye, A.S., Stevenson, L.M., Su, Y., Nisbet, R.M., Zhang, Y., Keller, A.A., 2016.
460 Influence of phytoplankton on fate and effects of modified zerovalent iron nanoparticles.
461 Environ. Sci. Technol. 50, 5597–605.

462 Auffan, M., Achouak, W., Rose, J., Roncato, M.A., Chanéac, C., Waite, D.T., Masion, A.,
463 Woicik, J.C., Wiesner, M.R., Bottero, J.Y., 2008. Relation between the redox state of
464 iron-based nanoparticles and their cytotoxicity toward *Escherichia coli*. Environ. Sci.
465 Technol. 42, 6730–6735.

466 Bardos, P., Bone, B., Černík, M., Elliott, D.W., Jones, S., Merly, C., 2015. Nanoremediation
467 and international environmental restoration markets. Remediat. J. 26, 101–108.

468 Bleyl, S., Kopinke, F.D., Mackenzie, K., 2012. Carbo-Iron-Synthesis and stabilization of
469 Fe(0)-doped colloidal activated carbon for in situ groundwater treatment. Chem. Eng. J.
470 191, 588–595.

471 Bosch, J., Heister, K., Hofmann, T., Meckenstock, R.U., 2010. Nanosized iron oxide colloids
472 strongly enhance microbial iron reduction. Appl. Environ. Microbiol. 76, 184–189.

473 Bouldin, J.L., Ingle, T.M., Sengupta, A., Alexander, R., Hannigan, R.E., Buchanan, R.A.,
474 2008. Aqueous Toxicity and Food Chain Transfer of Quantum Dots^{TM} in Freshwater
475 Algae and *Ceriodaphnia Dubia*. Environ. Toxicol. Chem. 27, 1958.

476 Cheloni, G., Cosio, C., Slaveykova, V.I., 2014. Antagonistic and synergistic effects of light
477 irradiation on the effects of copper on *Chlamydomonas reinhardtii*. Aquat. Toxicol.
478 155C, 275–282.

479 Cheloni, G., Marti, E., Slaveykova, V.I., 2016. Interactive effects of copper oxide
480 nanoparticles and light to green alga *Chlamydomonas reinhardtii*. Aquat. Toxicol. 170,

481 120–128.

482 Cheloni, G., Marti, E., Slaveykova, V.I., von Moos, N., Maillard, L., Slaveykova, V.I.,
483 Regier, N., Cosio, C., von Moos, N., Slaveykova, V.I., 2015. Interactive effects of
484 copper oxide nanoparticles and light to green alga *Chlamydomonas reinhardtii*. Aquat.
485 Toxicol. 170, 120–128.

486 Cooper, D.C., Picardal, F.W., Schimmelmann, A., Coby, A.J., 2003. Chemical and biological
487 interactions during nitrate and goethite reduction by *Shewanella putrefaciens* 200. Appl.
488 Environ. Microbiol. 69, 3517–3525.

489 Crane, R.A., Scott, T.B., 2012. Nanoscale zero-valent iron: Future prospects for an emerging
490 water treatment technology. J. Hazard. Mater. 211–212, 112–125.

491 Davies, K.J., 2000. Oxidative stress, antioxidant defenses, and damage removal, repair, and
492 replacement systems. IUBMB Life 50, 279–289.

493 Franqueira, D., Orosa, M., Torres, E., Herrero, C., Cid, a, 2000. Potential use of flow
494 cytometry in toxicity studies with microalgae. Sci. Total Environ. 247, 119–126.

495 Gillies, G., Mackenzie, K., Kopinke, F.D., Georgi, A., 2016. Fluorescence labelling as tool
496 for zeolite particle tracking in nanoremediation approaches. Sci. Total Environ. 550,
497 820–826.

498 Gillies, G., Rukmini, R., Kopinke, F.-D., Georgi, A., 2017. Suspension stability and mobility
499 of Trap-Ox Fe-zeolites for in-situ nanoremediation. J. Colloid Interface Sci. 501, 311–
500 320.

501 Gonzalez-Olmos, R., Kopinke, F.D., Mackenzie, K., Georgi, A., 2013. Hydrophobic Fe-
502 zeolites for removal of MTBE from water by combination of adsorption and oxidation.
503 Environ. Sci. Technol. 47, 2353–2360.

504 Gonzalez-Olmos, R., Roland, U., Toufar, H., Kopinke, F.D., Georgi, A., 2009. Fe-zeolites as
505 catalysts for chemical oxidation of MTBE in water with H_2O_2. Appl. Catal. B Environ.

506 89, 356–364.

507 Guillard, R.R.L., J.Lorenzen, C., 1972. Yellow-green algae with chlorophyllid C. J. Phycol.

508 He, W., Feng, Y., Li, X., Wei, Y., Yang, X., 2008. Availability and toxicity of Fe(II) and
509 Fe(III) in Caco-2 cells. J. Zhejiang Univ. Sci. B 9, 707–712.

510 Hjorth, R., Coutris, C., Nguyen, N., Sevcu, A., Baun, A., Joner, E., 2017. Ecotoxicity testing
511 and environmental risk assessment of iron nanomaterials for sub-surface remediation –
512 Recommendations from the FP7 project NanoRem. chemo 182, 525–531.

513 Keller, A. a., Garner, K., Miller, R.J., Lenihan, H.S., 2012. Toxicity of nano-zero valent iron
514 to freshwater and marine organisms. PLoS One 7, 1–10.

515 Klaine, S.J., Alvarez, P.J.J., Batley, G.E., Fernandes, T.F., Handy, R.D., Lyon, D.Y.,
516 Mahendra, S., McLaughlin, M.J., Lead, J.R., 2008. Nanomaterials in the environment:
517 behavior, fate, bioavailability, and effects. Environ. Toxicol. Chem. 27, 1825–1851.

518 Köber, R., Hollert, H., Hornbruch, G., Jekel, M., Kamptner, a., Klaas, N., Maes, H.,
519 Mangold, K.-M., Martac, E., Matheis, a., Paar, H., Schäffer, a., Schell, H., Schiwy, a.,
520 Schmidt, K.R., Strutz, T.J., Thümmler, S., Tiehm, a., Braun, J., 2014. Nanoscale zero-
521 valent iron flakes for groundwater treatment. Environ. Earth Sci. 72, 3339–3352.

522 Lee, C., Kim, J.Y., Lee, W. Il, Nelson, K.L., Yoon, J., Sedlak, D.L., 2008. Bactericidal effect
523 of zero-valent iron nanoparticles on *Escherichia coli*. Env. Pollut 13, 4927–4933.

524 Lei, C., Zhang, L., Yang, K., Zhu, L., Lin, D., 2016. Toxicity of iron-based nanoparticles to
525 green algae: Effects of particle size, crystal phase, oxidation state and environmental
526 aging. Environ. Pollut. 218, 505–512.

527 Mackenzie, K., Bleyl, S., Georgi, A., Kopinke, F.D., 2012. Carbo-Iron - An Fe/AC composite
528 - As alternative to nano-iron for groundwater treatment. Water Res. 46, 3817–3826.

529 Mackenzie, K., Bleyl, S., Kopinke, F.D., Doose, H., Bruns, J., 2016. Carbo-Iron as
530 improvement of the nanoiron technology: From laboratory design to the field test. Sci.

Total Environ. 563–564, 641–648.

Maxwell, K., Johnson, G.N., 2000. Chlorophyll fluorescence--a practical guide. J. Exp. Bot. 51, 659–668.

Messerli, M. a, Amaral-Zettler, L. a, Zettler, E., Jung, S.-K., Smith, P.J.S., Sogin, M.L., 2005. Life at acidic pH imposes an increased energetic cost for a eukaryotic acidophile. J. Exp. Biol. 208, 2569–79.

Mueller, N.C., Braun, J., Bruns, J., Černík, M., Rissing, P., Rickerby, D., Nowack, B., 2012. Application of nanoscale zero valent iron (NZVI) for groundwater remediation in Europe. Environ. Sci. Pollut. Res. 19, 550–558.

Pavlíková, S., Šerše, F., Jesenák, K., Gáplovská, K., Gabriel, Č., 2010. Efficacy of modified natural zeolites in the protection against the damaging effect of 4-chlorophenol on algal growth. Fresenius Environ. Bull. 19, 3055–3058.

Ribas, D., Cernik, M., Martí, V., Benito, J.A., 2016. Improvements in nanoscale zero-valent iron production by milling through the addition of alumina. J. Nanoparticle Res. 18, 181.

Hjorth, R., Sørensen, S.N., Olsson, M.E., Baun, A., Hartmann, N.B., 2015. A certain shade of green: Can algal pigments reveal shading effects of nanoparticles? Integr. Environ. Assess. Manag. 11, 719–728.

Schiwy, A., Maes, H.M., Koske, D., Flecken, M., Schmidt, K.R., Schell, H., Tiehm, A., Kamptner, A., Thümmler, S., Stanjek, H., Heggen, M., Dunin-Borkowski, R.E., Braun, J., Schäffer, A., Hollert, H., 2016. The ecotoxic potential of a new zero-valent iron nanomaterial, designed for the elimination of halogenated pollutants, and its effect on reductive dechlorinating microbial communities. Environ. Pollut. 216, 1–9.

Schwab, F., Bucheli, T.D., Lukhele, L.P., Magrez, A., Nowack, B., Sigg, L., Knauer, K., 2011. Are carbon nanotube effects on green algae caused by shading and agglomeration? Environ. Sci. Technol. 45, 6136–6144.

556 Ševců, A., El-Temsah, Y.S., Joner, E.J., Černík, M., 2011. Oxidative stress induced in
557 microorganisms by zero-valent iron nanoparticles. Microbes Environ. 26, 271–281.

558 Sharma, V.K., Chen, L., Marsalek, B., Zboril, R., O'Shea, K.E., Dionysiou, D.D., 2016. Iron
559 based sustainable greener technologies to treat cyanobacteria and microcystin-LR in
560 water. Water Sci. Technol. Water Supply 1–9.

561 Sørensen, S.N., Engelbrekt, C., Lützhøft, H.H., Jiménez-Lamana, J., Noori, J.S., Alatraktch,
562 F.A., Delgado, C.G., Slaveykova, V.I., Baun, A., 2016. A multi-method approach for
563 disclosing algal toxicity of platinum nanoparticles. Environ. Sci. Technol. 19, 10635–
564 10643.

565 Soukupova, J., Zboril, R., Medrik, I., Filip, J., Safarova, K., Ledl, R., Mashlan, M., Nosek, J.,
566 Cernik, M., 2015. Highly concentrated, reactive and stable dispersion of zero-valent iron
567 nanoparticles: Direct surface modification and site application. Chem. Eng. J. 262, 813–
568 822.

569 Szivák, I., Behra, R., Sigg, L., 2009. Metal-induced reactive oxygen species production in
570 *Chlamydomonas reinhardtii* (Chlorophyceae). J. Phycol. 45, 427–435.

571 Vardanyan, Z., Trchounian, A., 2012. Fe(III) and Fe(II) ions different effects on Enterococcus
572 hirae cell growth and membrane-associated ATPase activity. Biochem. Biophys. Res.
573 Commun. 417, 541–545.

574 Velásquez, M., Santander, I.P., Contreras, D.R., Yáñez, J., Zaror, C., Salazar, R. a, Pérez-
575 Moya, M., Mansilla, H.D., 2014. Oxidative degradation of sulfathiazole by Fenton and
576 photo-Fenton reactions. J. Environ. Sci. Health. A. Tox. Hazard. Subst. Environ. Eng.
577 49, 661–670.

578 von Moos, N., Maillard, L., Slaveykova, V.I., 2015. Dynamics of sub-lethal effects of nano-
579 CuO on the microalga *Chlamydomonas reinhardtii* during short-term exposure. Aquat.
580 Toxicol. 161, 267–275.

581 Wang, G., Li, X., Fang, Y., Huang, R., 2014. Analysis on the formation condition of the
582 algae-induced odorous black water agglomerate. Saudi J. Biol. Sci. 21, 597–604.

583 Zhu, X., Tian, S., Cai, Z., 2012. Toxicity assessment of iron oxide nanoparticles in Zebrafish
584 (*Danio rerio*) early life stages. PLoS One 7, 1–6.

585

Table 1. Z-averaged particle size determined in algal growth medium after 2h and 24h. The results are average of three replicated experiments.

	Z-average size after 2h (nm ± SD)		
particles	**10 mg L^{-1}**	**50 mg L^{-1}**	**500 mg L^{-1}**
FerMEG12	4076 ± 320	3726 ± 580	4608 ± 243
Carbo-Iron®	2874 ± 1005	1515 ± 183	1289 ± 26
Fe-zeolites	845 ± 114	810 ± 88	789 ± 41
Nano-Goethite	254 ± 1	288 ± 80	233 ± 11
	Z-average size after 24h (nm ± SD)		
FerMEG12	4974 ± 1426	4721 ± 380	4426 ± 340
Carbo-Iron®	2037 ± 656	1643 ± 174	1326 ± 16
Fe-zeolites	977 ± 420	798 ± 114	856 ± 58
Nano-Goethite	207 ± 3	251 ± 6	245 ± 2

Figures

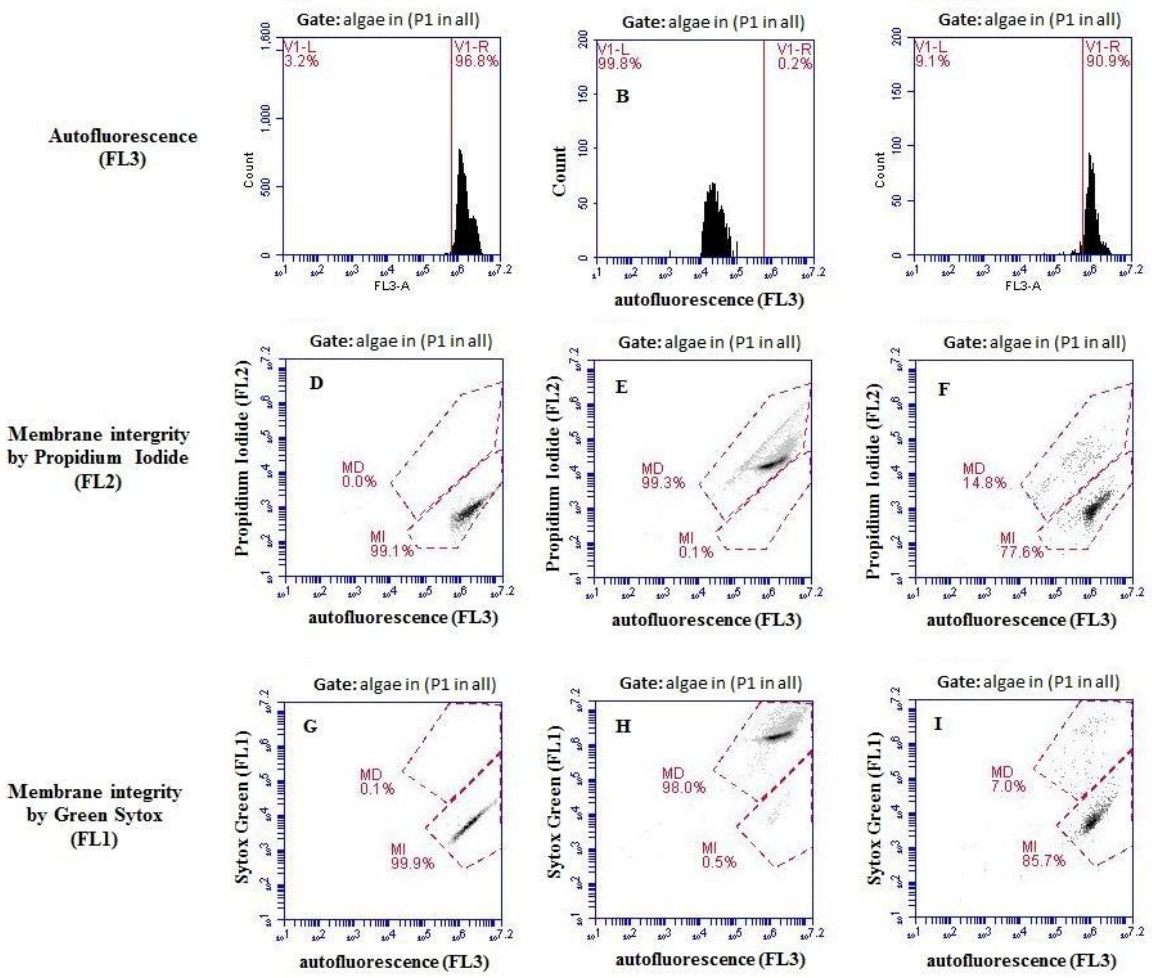

Fig. 1. FCM gating strategy to distinguish particles, damaged (MD) and unaffected cells (MI). Autofluorescence was measured with fluorescence channel 3 (FL3), membrane integrity (MI)/membrane damage (MD) using the fluorescent probe propidium iodide in fluorescence channel 2 (FL2) and using the fluorescent probe Green Sytox in channel 1 (FL1), as visualized above. The first column is algal culture only (negative control), second column is heated algae (positive control) and third column is algae exposed to the particles.

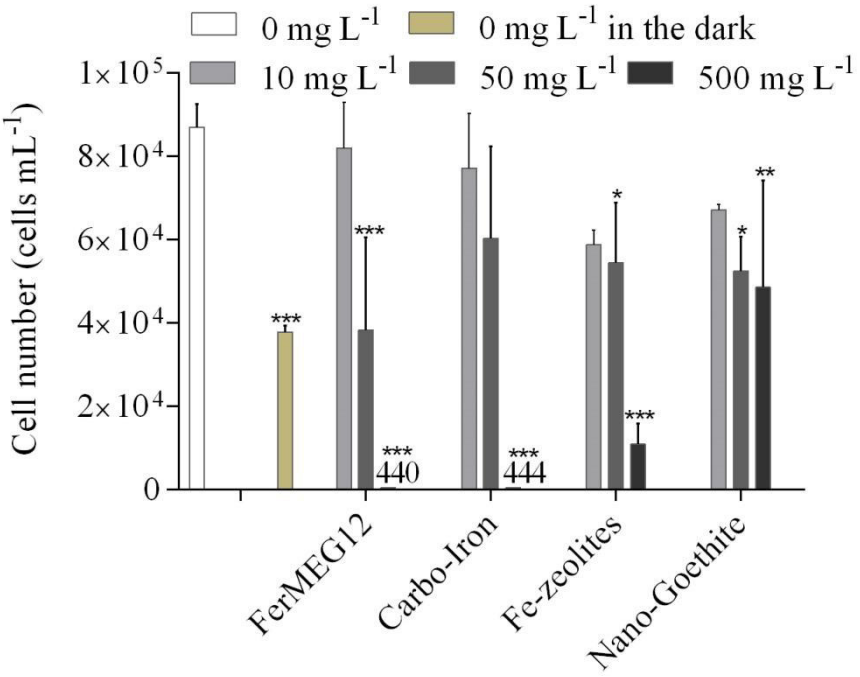

Fig. 2. Effect of four particle types on number of algal cells mL^{-1} measured with FCM. Exposure conditions: FerMEG12, Carbo-Iron®, Fe-zeolites and Nano-Goethite at concentrations of 10, 50, 500 mg L^{-1}. The error bars represent the standard deviation of triplicate samples. Significance levels * $P < 0.05$, ** $P < 0.01$, and *** $P < 0.001$.

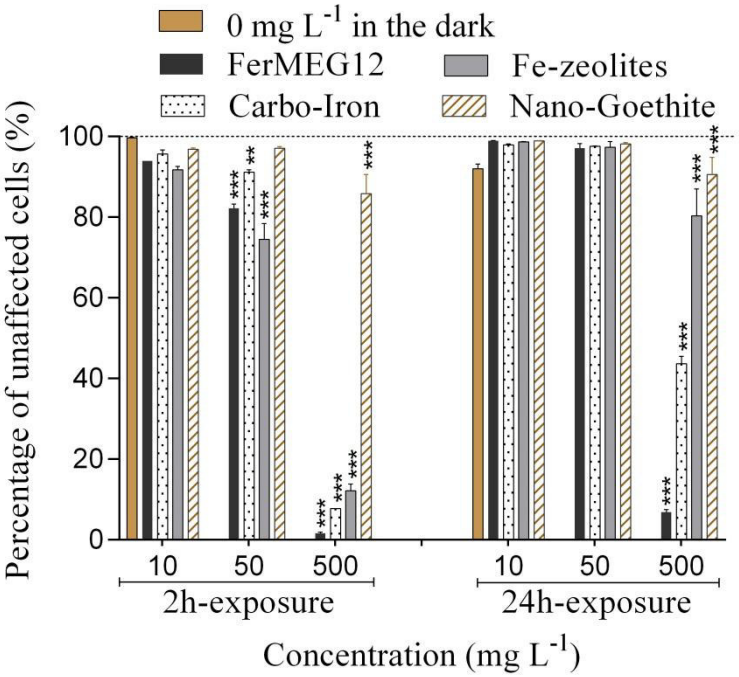

Fig. 3. Effect of particle exposure on the chlorophyll fluorescence of *Chlamydomonas* cells. Exposure conditions: FerMEG12, Carbo-Iron®, Fe-zeolites and Nano-Goethite at concentrations of 10, 50, 500 mg L^{-1}, duration 2 h and 24 h. The chlorophyll fluorescence of unexposed control represents 100 %. The error bars represent the standard deviation of triplicate samples. Significance levels * $P < 0.05$, ** $P < 0.01$, and *** $P < 0.001$.

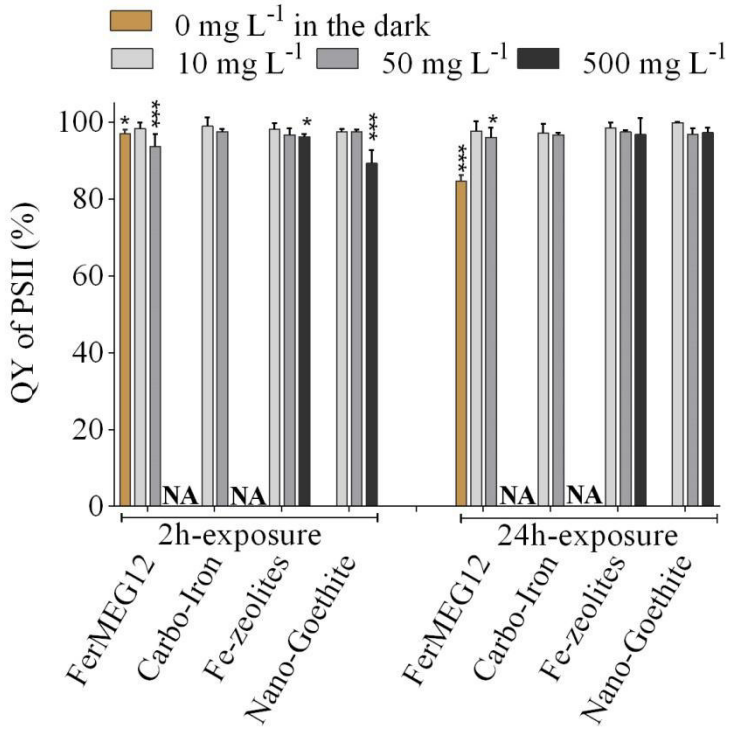

Fig. 4. Effect of particles on the quantum yield (QY) of photosystem II (%) of *Chlamydomonas* after 2 h and 24 h exposure to Fe-NMs at 0, 10 and 50 mg L^{-1} (FerMEG12, Carbo-Iron®) and 0, 10, 50 and 500 mg L^{-1} (Fe-zeolites, Nano-Goethite). Grey bars are control algae grown without nanoparticles in the dark. The control without particles represents 100 %. NA = not analyzed as the dark color induced by the particle suspensions interfered with measurement. The error bars represent the standard deviation of triplicate samples. Significance levels * $P < 0.05$, ** $P < 0.01$, and *** $P < 0.001$.

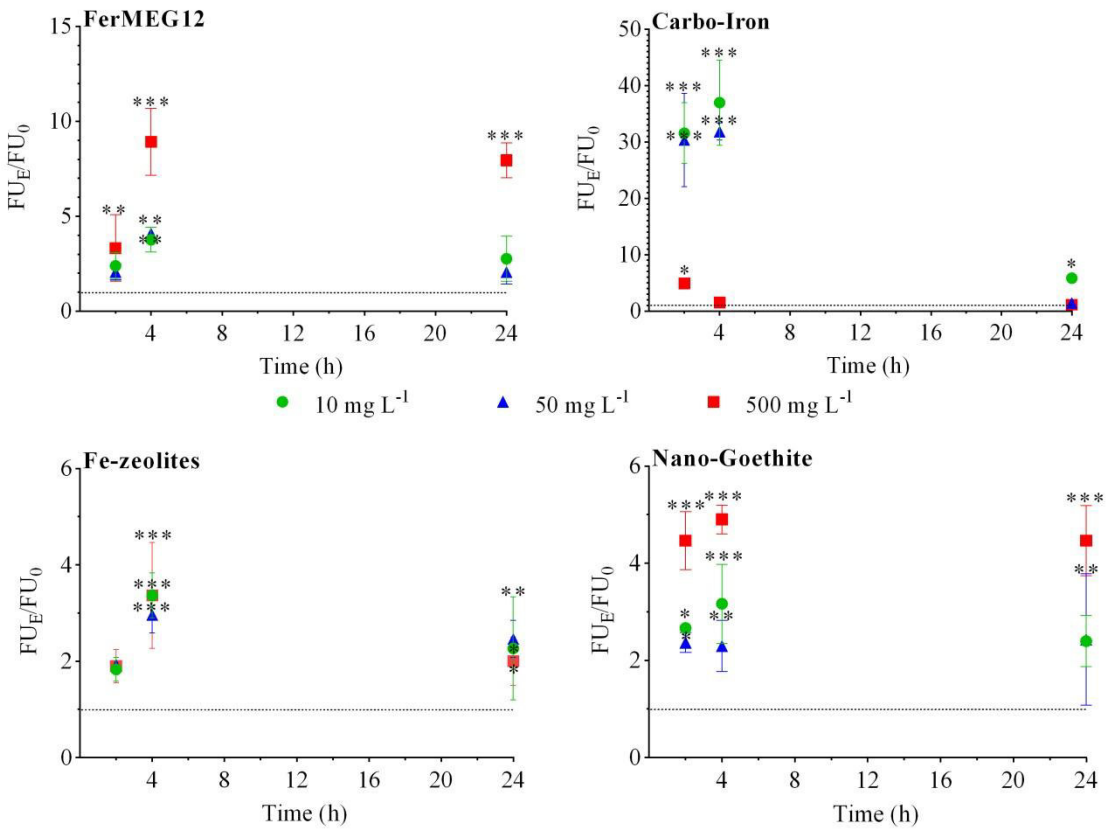

Fig. 5. Fluorescence unit (FU) ratios (FU_E/FU_0) of ROS production in *Chlamydomonas* cells after 2 h, 4 h and 24 h exposure to FerMEG12, Carbo-Iron®, Fe-zeolites and Nano-Goethite at concentrations of 10 (green circle), 50 (blue up-triangle) and 500 (red square) mg L^{-1}. FU_E: florescence unit of exposed algae to Fe-NMs, FU_0: non-exposed *Chlamydomonas* cultures. The dotted line (---) represents the control and the error bars represent the standard deviation of triplicate samples. Note the different y-axis scales. Significance levels * $P < 0.05$, ** $P < 0.01$, and *** $P < 0.001$.

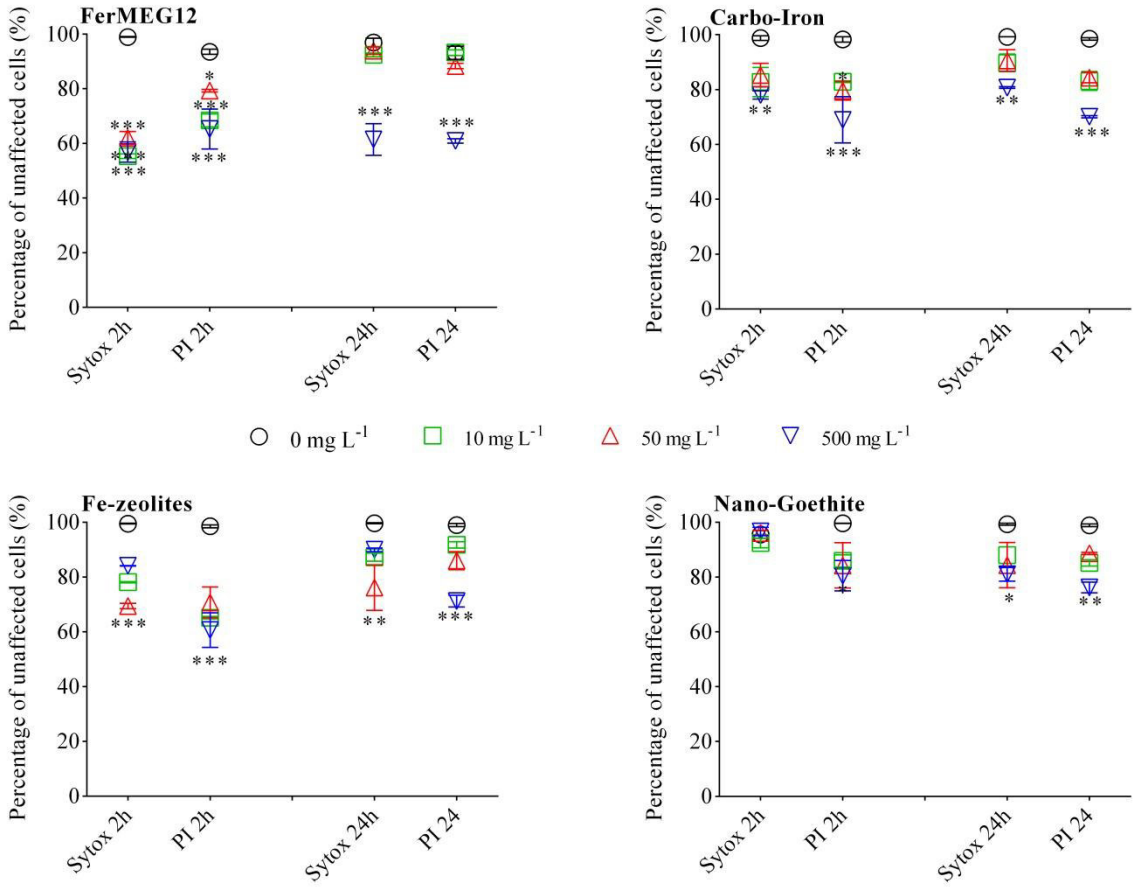

Fig. 6. Influence of the four particle types on the membrane integrity of *Chlamydomonas* cells after 2 h and 24 h exposure to FerMEG12, Carbo-Iron®, Fe-zeolites and Nano-Goethite at concentrations of 10 (green square), 50 (red up-triangle) and 500 mg L^{-1} (blue down-triangle). The error bars represent the standard deviation of triplicate samples. Significance levels * $P < 0.05$, ** $P < 0.01$, and *** $P < 0.001$.

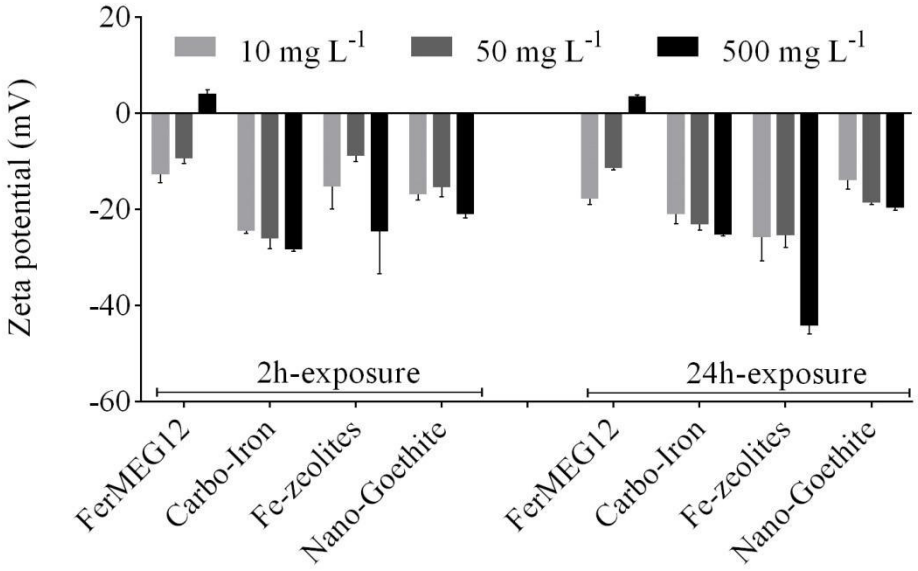

Fig. 7. Zeta-potential of particle surfaces at different concentrations after 2 h and 24 h dispersed in algal growth medium. Error bars = standard deviation of triplicate samples.

Supplementary Material

Biological effect of four iron-containing materials developed for nanoremediation on green alga *Chlamydomonas* sp.

[a]Nhung H. A. Nguyen, [b]Nadia R. von Moos, [b]Vera I. Slaveykova*, [c]Katrin Mackenzie, [d]Rainer U. Meckenstock, [e]Silke Thümmler, [f,1]Julian Bosch, and [a]Alena Ševců*

[a]Technical University of Liberec; Institute for Nanomaterials, Advanced Technologies and Innovation; Faculty of Mechatronics, Informatics and Multidisciplinary Studies; Studentská 2, 461 17 Liberec, Czech Republic, nhung.nguyen@tul.cz, alena.sevcu@tul.cz

[b]University of Geneva, Faculty of Sciences, Earth and Environmental Sciences, Department for Environmental and aquatic sciences, Uni Carl Vogt, 66 Bvd Carl Vogt, 1211 Geneva, Switzerland, vera.slaveykova@unige.ch, nadia.vonmoos@immerda.ch

[c]Helmholtz Centre for Environmental Research GmbH-UFZ, Permoserstraße 15, 04318 Leipzig, Germany. katrin.mackenzie@ufz.de

[d]University of Duisburg-Essen, Biofilm Centre, Universitätsstr. 5, 45141 Essen, Germany. rainer.meckenstock@uni-due.de

[e]Verfahrensentwicklung Umweltschutztechnik Recycling GmbH, Chemnitzer Straße 40,09599 Freiberg, Germany. Silke.Thuemmler@mvtat.tu-freiberg.de

[f]Helmholtz Zentrum München, Ingolstädter Landstraße 1, D-85764 Neuherberg, Germany.

[1]Present address: Intrapore UG, Katernberger Str. 107, 45327 Essen, Germany. julian.bosch@intrapore.com

*corresponding authors: alena.sevcu@tul.cz; vera.slaveykova@unige.ch

CONTENTS

MATERIAL AND METHODS

RESULTS

Figure S7. Size distribution based on scattered light intensity and number of Fe materials at 2h and 24h in Guillard-Lorenzen algal growth medium: FerMEG12 (A), (B); Carbo-Iron® (C), (D); Fe-zeolites (E), (F); and Nano-Goethite (G), (H). Data obtained using dynamic light scattering (DLS).

Figure S8. pH (A) and oxidative/reductive potential (ORP) (B) of *Chlamydomonas* in Guillard-Lorenzen algal growth medium exposed to different nanoparticles at concentrations of 0, 10, 50 and 500 mg L^{-1} at 0h and after 24 hours. The error bars represent the standard deviation of duplicate measurements.

REFERENCE

Guillard, R. R. L. & Lorenzen, C. J. (1972). Yellow-green algae with chlorophyllid C. Phycology.

MATERIAL AND METHODS

Table S1. Guillard-Lorenzen algal growth medium (Guillard and Lorenzen 1972).

	Ingredients	Concentration (g L^{-1})
1	$CaCl_2 \cdot 2H_2O$	36.8
2	$MgSO_4 \cdot 7H_2O$	37
3	$NaHCO_3$	12.6
4	$K_2HPO_4 \cdot 3H_2O$	5.7
5	$NaNO_3$	42.5
6	$Na_2SiO_3 \cdot 5H_2O$	21.2
7	Na_2EDTA	4.36
8	$FeCl_3 \cdot 6H2O$	3.15
9	$CuSO_4 \cdot 5H_2O$	0.01
10	$ZnSO_4 \cdot 7H_2O$	0.022
11	$CoCl_2 \cdot 6H_2O$	0.01
12	$MnCl_2 \cdot 4H_2O$	0.18
13	$Na_2MoO_4 \cdot 2H_2O$	0.006
14	H_3BO_3	1
15	Thiamine	0.1
16	Biotine	0.0005
17	Cyanocobalamine	0.0005
18	TRIS-hydrochloride	0.115

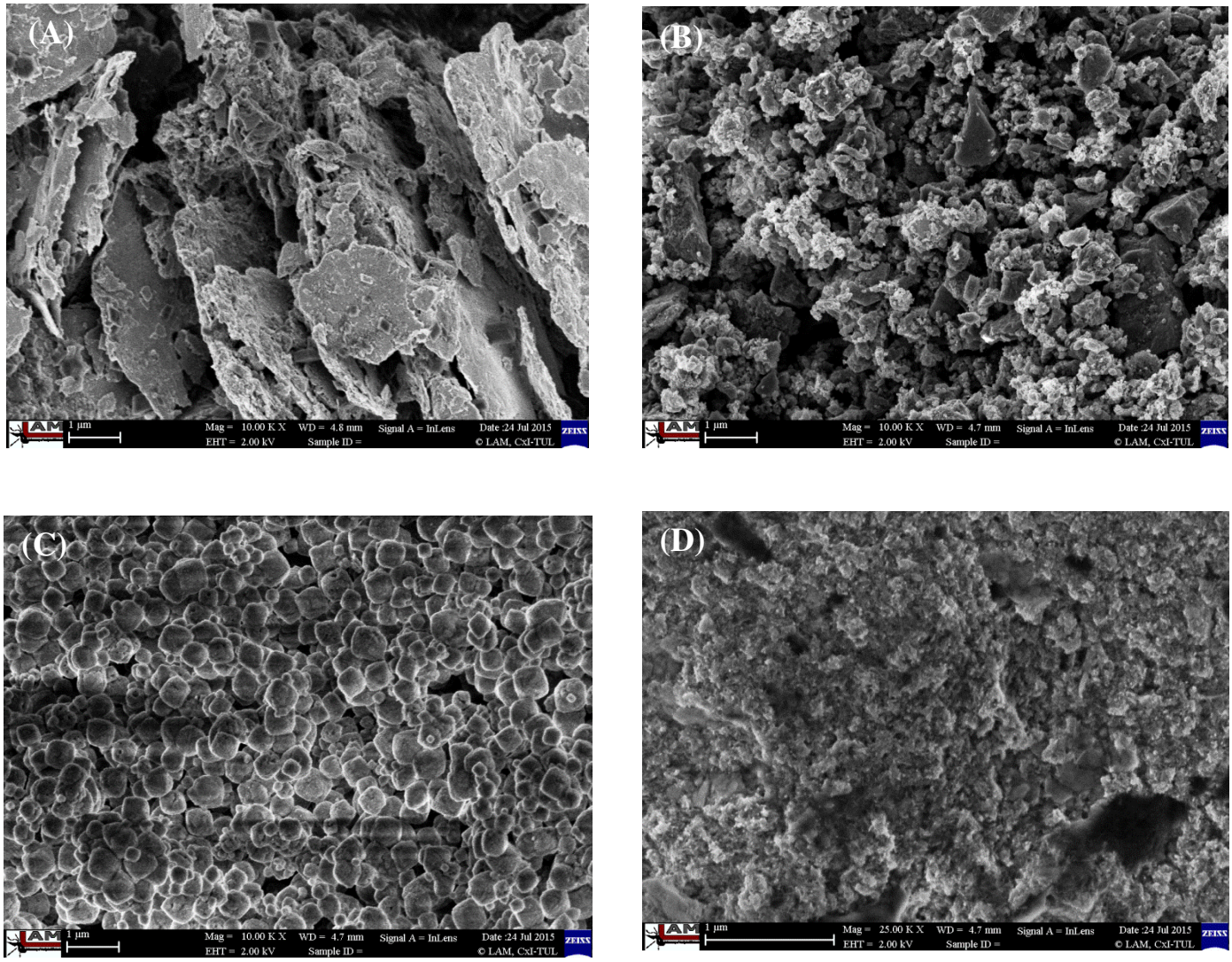

Figure S1. Pristine dry particle types: (A) FerMEG12, (B) Carbo-Iron®, (C) Fe-zeolites, and (D) Nano-Goethite. Images obtained using scanning electron microscopy.

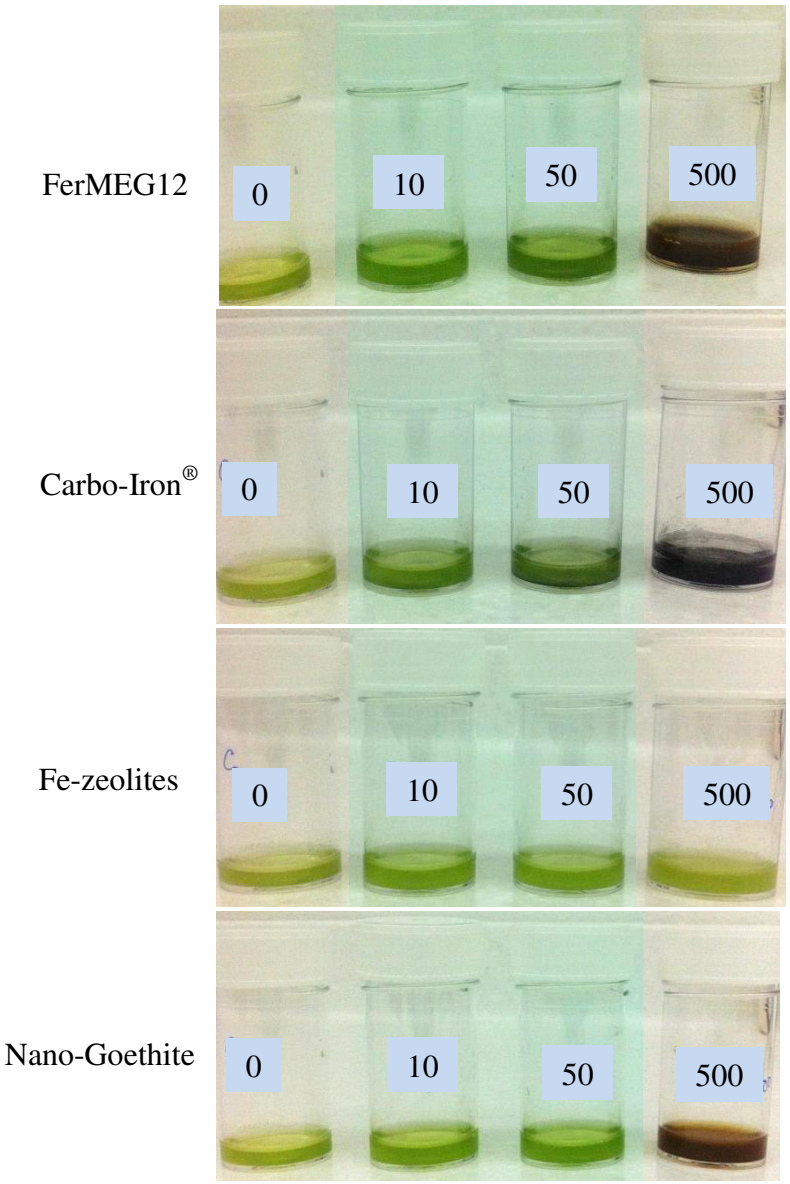

Figure S2. Example images of *Chlamydomonas* culture after 24 h exposure to 5 to 500 mg L^{-1} of: FerMEG12 (1st row), Carbo-Iron® (2nd row), Fe-zeolites (3rd row) and Nano-Goethite (4th row). The brownish colour of the FerMEG12 shows oxidation of the particles surface to iron oxides.

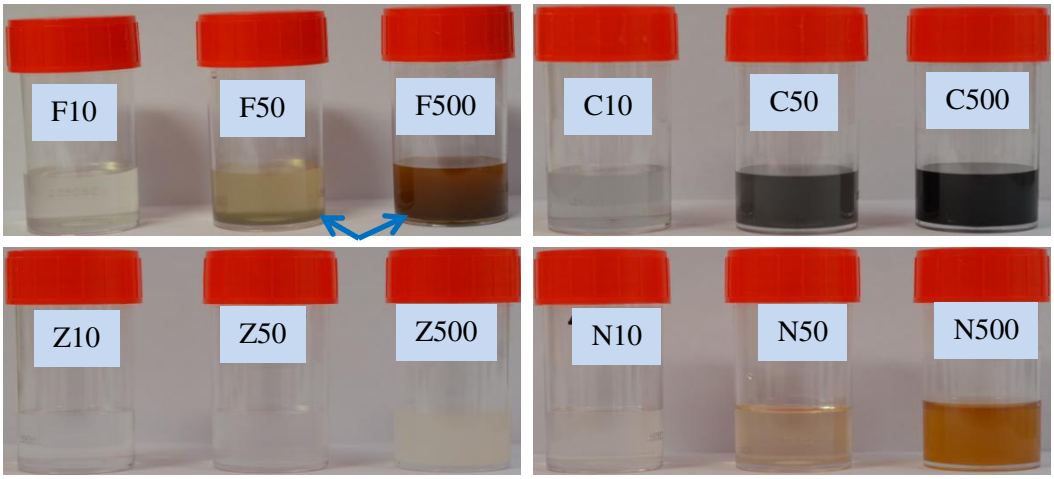

Figure S3. Photos of particle suspensions (10, 50 and 500 mg L^{-1}) in agal medium after 24 h on the shaker. F: FerMEG12, C: Carbo-Iron®, Z: Fe-zeolites, N: Nano-Goethite. Blue arrows indicate the samples with sediment formation.

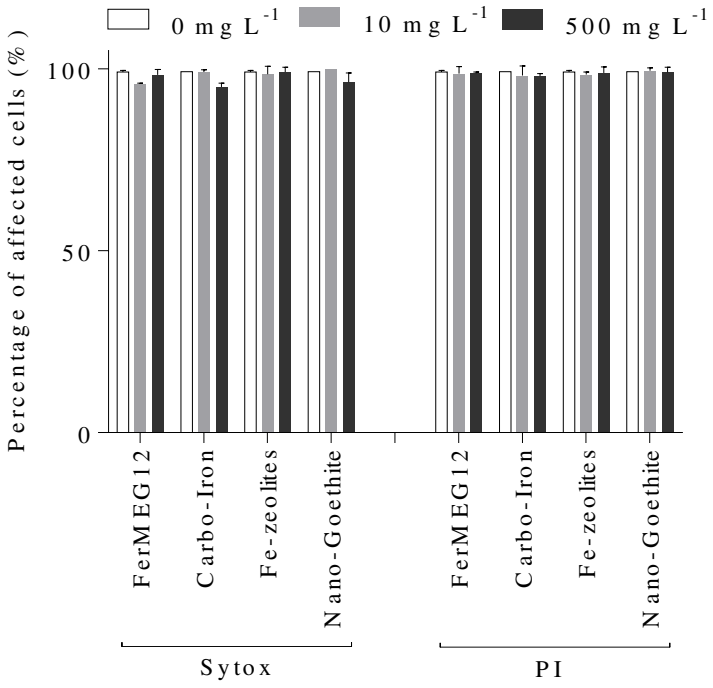

Figure S4. Reference controls to test if the probes did not interfere with Fe materials. Samples of Fe materials (10 and 500 mg L^{-1}) were incubated with Sytox Green and propidium iodide (PI) probes for 15 minutes in darkness and then centrifuged for 10 minutes at 4°C. The supernatant with the fluorescent probes was then used to stain the hot-water treated cells. The percentage of affected cells was analysed using the flow cytometer stategy illustrated in Figure 1.

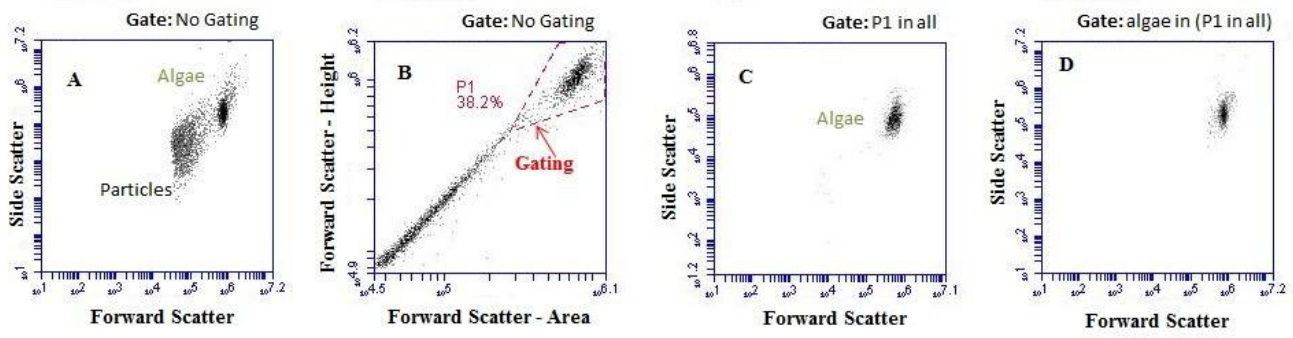

Figure S5. Example of FCM gating strategy. A) raw data, B) removing doublets with gate "P1" (FSC-A vs FSC-H) (Gating), C) algae gate in P1 gated scatter plot of algae culture (FSC vs SSC) and D) "cleaned" data set: raw data gated on "algae in (P1 in all) (FSC vs SSC).

RESULTS

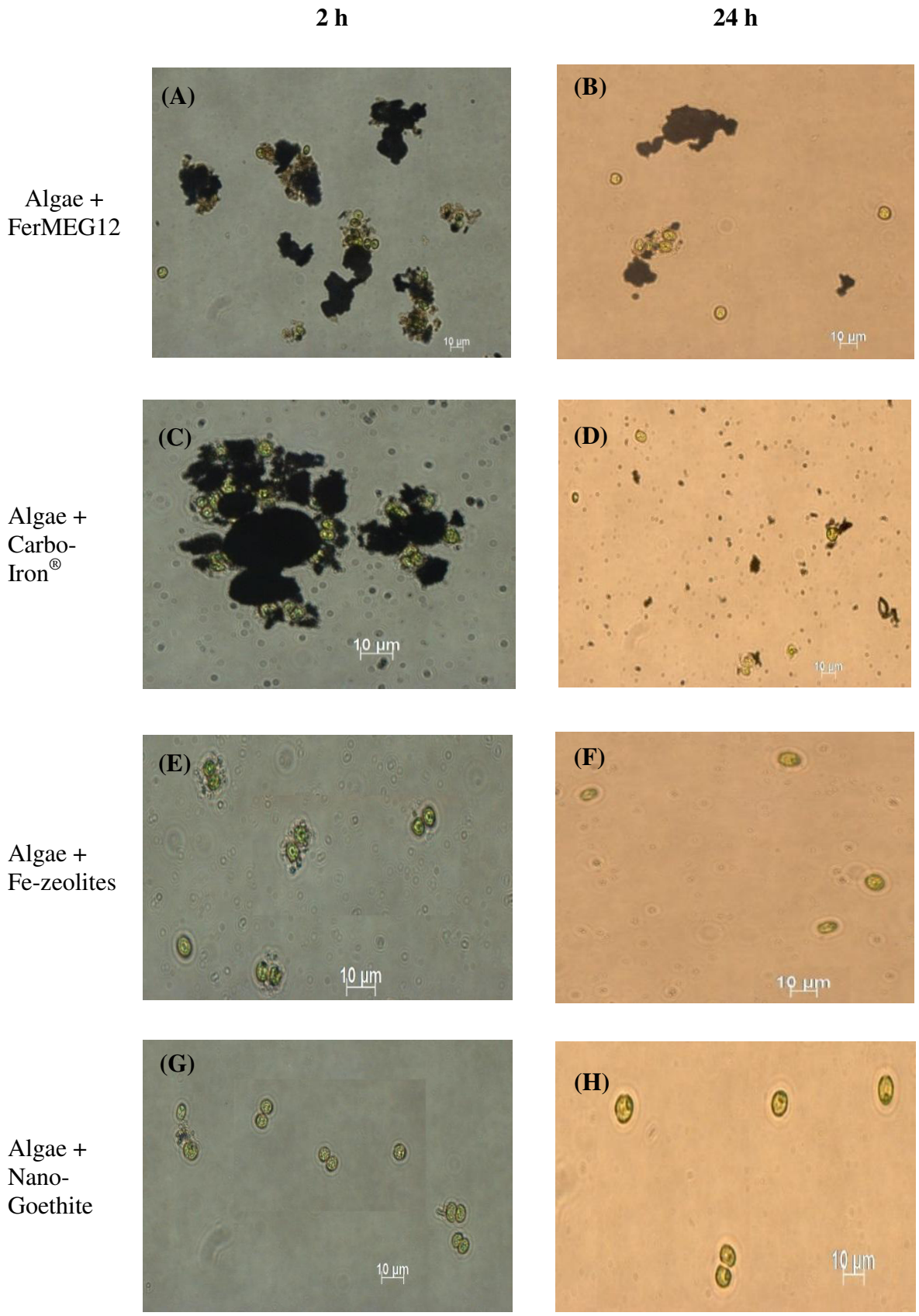

Figure S6. *Chlamydomonas* culture after 2 h and 24 h exposure to 500 mg L^{-1} of: FerMEG12 (A, B), Carbo-Iron® (C, D), Fe-zeolites (E, F) and Nano-Goethite (G, H). Images were taken using a bright field Zeiss microscope (mag. 400 x; scale bar = 10 µm).

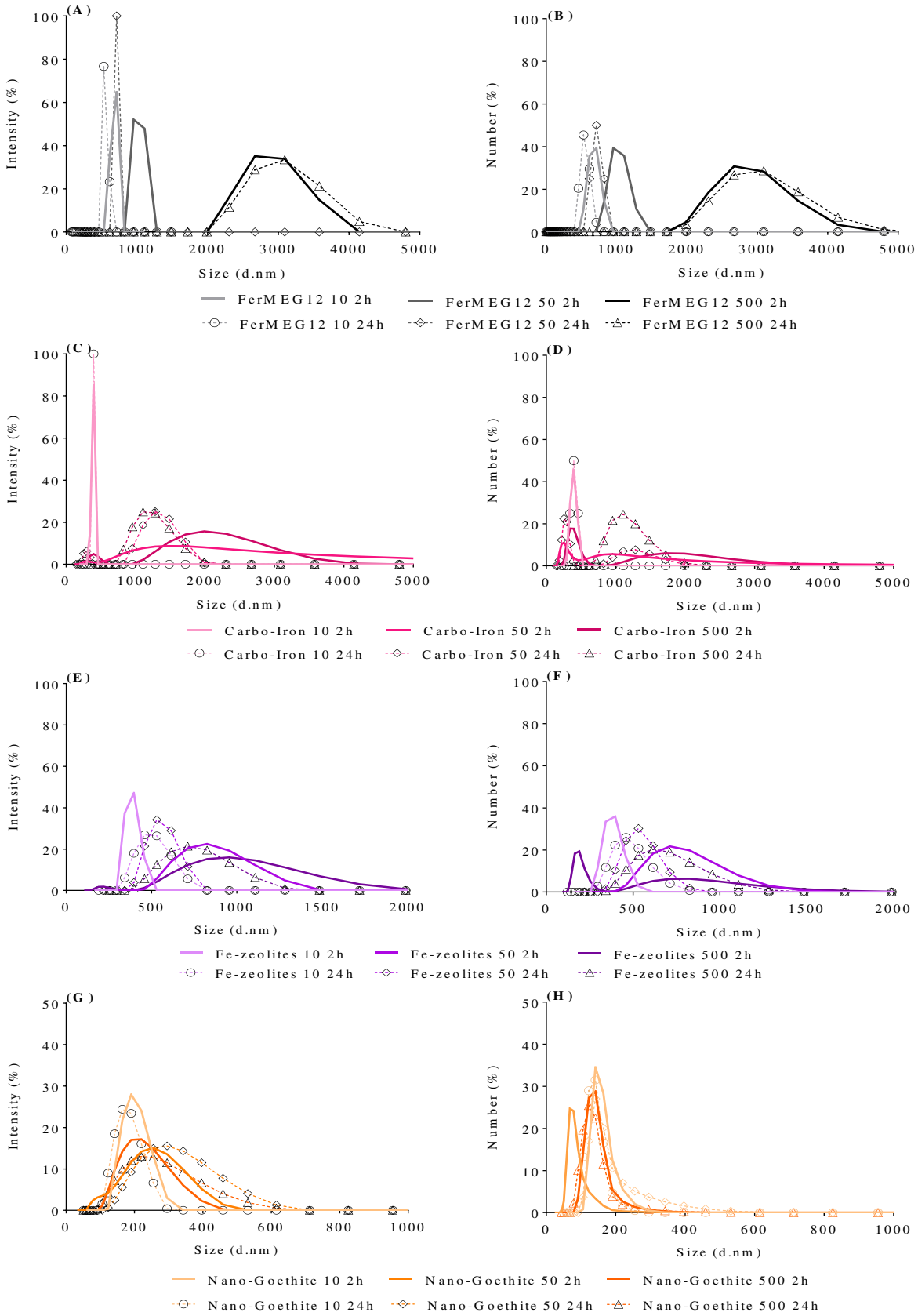

Figure S7. Size distribution based on scattered light intensity (%) and number (%) of particles at 2 h and 24 h in Guillard-Lorenzen algal growth medium: FerMEG12 (A), (B); Carbo-Iron® (C), (D); Fe-zeolites (E), (F); and Nano-Goethite (G), (H). Number 10, 50 and 500 in the graphs were concentrations (mg L^{-1}) of particles. Data obtained using dynamic light scattering (DLS).

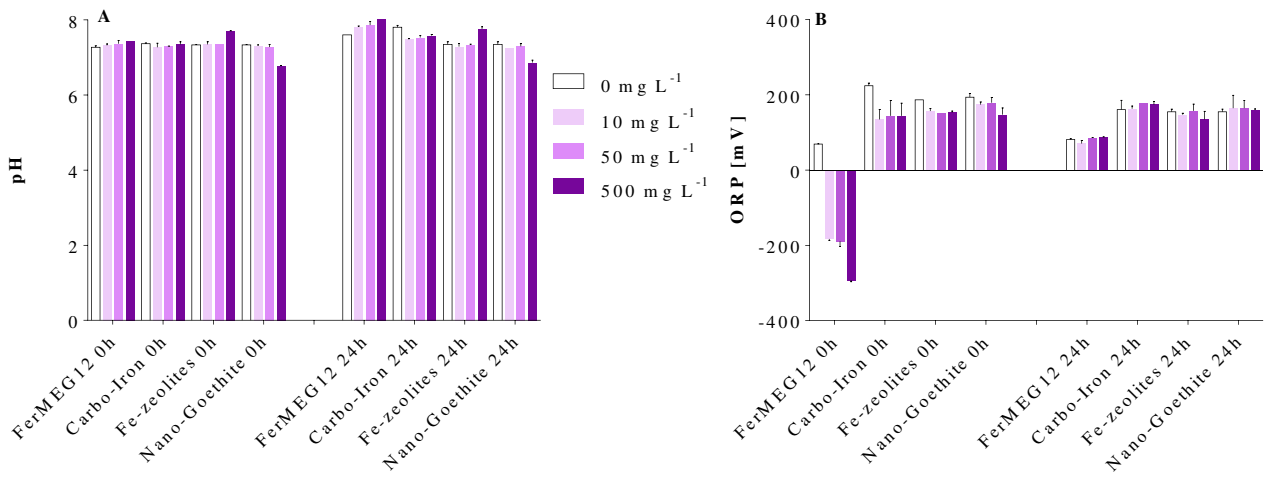

Figure S8. pH (A) and oxidative/reductive potential (ORP) (B) of *Chlamydomonas* in algal growth medium exposed to different nanoparticles at concentrations of 0, 10, 50 and 500 mg L^{-1} at 0h and after 24 hours. The error bars represent the standard deviation of duplicate measurements.